

Pin-point effect determination using a rigorous approach

Mehran Dadgar¹, S Mohammad Hosseini Varkiyani^{1,a} & Ali Akbar Merati²

¹Textile Engineering Department, ²Advanced Textile Materials and Technology Research Institute,
Amirkabir University of Technology, 424 Hafez Street, Tehran, Iran

Received 6 February 2014; Revised received and accepted 23 May 2014

A new method for evaluating the pin-point effect of pile yarn of carpets before weaving has been introduced. The method has been initially accomplished by presenting a standard method for bundle preparation and consequently the pin-point index is presented by image analysis technique. To this end, yarns with different twists are heat set at various times and temperatures. Comparison of the results shows that increasing the twist, time and temperature positively contribute to the pin-point index. In the last section, an adaptive neuro fuzzy model (ANFIS) and an artificial neural network model (ANN) have been designed to predict the pin-point index of the heat set yarns based on training with the experimental data. The input parameters are twist, time and temperature, and the output is the pin-point index. The results illustrate that the learning capability of the ANFIS model is superior and its generalization ability is slightly better than that of a standalone ANN model.

Keywords: Adaptive neuro network, Heat setting, Neuro fuzzy inference system, Pin-point effect, Tip definition, Tip effect

Introduction

Pin-point effect is one of the most common user-friendly effects that appears after heat setting on the carpet appearance. This effect makes the carpets more beautiful with a better appearance. Everaert *et al.*¹ used the word ‘tip definition’ and ‘tip effect’ instead of pin-point effect in their study. Afterwards, superba and power heat set named the tip effect as ‘pin-point effect’. In a carpet, a heat-set pile has a close packed structure, the same as a pin or needle. This effect is called the pin-point effect. Higher pin-point effect means closer structure and higher packing density of a pile yarn. One of the most important aspects of this new structure is its durability which is achieved by good heat setting after cutting the piles². The pin-point effect emerges after the heat setting; thus it is very meaningful to review the literature of heat setting, which may not only find the relative information, but also at least may help to show the research lack in this field and understand more importance of the pin-point index. Heat setting plays an important role on the quality of textile products, because they take different stresses through spinning, weaving and finishing processes². It can remove or reduce these stresses and let the yarns be relaxed. Similarly, the time–temperature relationship

in the heat setting process varies, depending on the polymer, fabric weight and the basic construction³. Stattonet *et al.*² and Gupta⁴ classified the yarn heat-setting as the permanent setting, semi-permanent setting and temporary setting. This classification confirms the importance of heat setting in the textile industries. In fact, the textile materials receive the lowest level of energy after the permanent heat setting. There are many studies reported in the heat setting field with concentration on the physical and mechanical properties of the yarns⁵⁻⁹ and lot of researches are available on the polymer morphology after heat setting¹⁰⁻²³ using DSC, XRD, etc. for different fibres such as nylon, PET and PP. Despite the extensive researches on the effect of yarn and heat set parameters on the inner structure of heat set yarns, there exists less work on the investigation of the carpets appearance²⁴⁻³³. In most of these studies, the image analysis methods helped the researchers to identify the relationship between the carpet surface structure and the carpet appearance. They tried to find out the relationship between carpet texture changing and carpet wear, carpet appearance, surface intensity, surface roughness, carpet appearance retention, and carpet appearance loss. To the best of our knowledge, there exists no investigation that encompasses the pin-point effect and its evaluation²⁹. For instance, Xu³⁴ uses image analysis techniques for investigating carpet appearance retention. He also expanded the

^aCorresponding author.
E-mail: varkiyan@aut.ac.ir,

application of image analysis for assessing appearance change in tufted carpets by means of tuft characterization such as geometry, orientation, and spatial arrangements. Xu³⁴ further reviewed other studies that applied image analysis techniques on carpet appearance characteristics.

Literature review also clarify that there is no research work to introduce an index to quantitatively investigate and compare the pin-point effect of the carpets while the pin-point effect is an important parameter specifying the carpet appearance. Hence, in this research work, the pin-point index has been studied. Effort has been made to predict the pin-point index by using different models, being used for predicting the textile parameters. Ucar and Ertugrul³⁵ reported the prediction of bursting strength of the knitted fabrics by ANN and ANFIS approaches. Majumdar³⁶ utilized an adaptive neuro-fuzzy inference system for predicting the hairiness of cotton yarns. Other researchers tried to predict some parameters such as shrinkage by intelligence system³⁷⁻⁴¹. Lin²³ predicted the yarn shrinkage using ANN models. He finished woven fabrics and estimated the shrinkages of warp and weft yarns in the finished woven fabrics using ANN. In this study also, ANFIS and ANN have been developed to predict the pin-point index from the yarn twist, time and temperature parameters. In addition, statistical and graphical error analyses are also carried out for the accuracy and adequacy of the models.

2 Materials and Methods

Figure 1 shows the yarn structures before and after heat setting. The conventional industrial method for evaluating the appearance of pin-point effect is the subjective evaluation by expert observatory. While its prerequisite step is the carpet sampling, this procedure

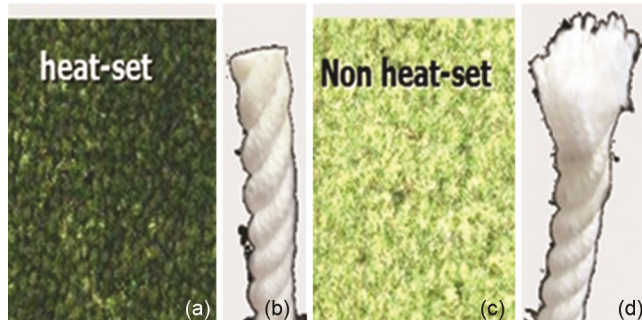


Fig. 1—Pin-point effect in heat-set and non-heat-set yarns (a) surface of heat-set piles, (b) heat-set yarn with good pin-point effect after cutting, (c) surface of non-heat-set piles and (d) non-heat-set yarn with a fluffly blown effect after cutting 42

can solely be applied repetitively. However, due to the weaving tension, pile cutting, temperature of sizing cylinder, cutter sharpness, and many other parameters, creating a constant condition is difficult and more or less impossible. Considering above, introducing an index to characterize the pin-point effect before the carpet production is more meaningful from the economic point of view. Due to the differences in yarn parameters such as twist, linear density, and material, a method is necessary for specifying the differences between yarn samples before introducing the pin-point index. Actually, a special standard method for the sample preparation is necessary to allow the experts to compare and evaluate the bundle yarns at a constant condition.

2.1 Standard Method for Bundle Yarns Preparation

Detecting the pin-point index from bundle yarns is easier than that from carpets, because of the easier sample preparation. As a result, it is necessary to define a new method to prepare a standard bundle for comparison with others. Since no standard method for the bundle preparation exists, designing a standard method is a primary step. To this end, it is prerequisite to know the suitable area of tube bundle, number of yarns placed in tube area, and finally assembling the method. Good understanding help us to compare the bundle yarns samples even at different linear densities. For the sample preparation, a certain number of threads in a given area and subsequently the total density of yarn’s surface are required. This is similar to the bundle cross section. Afterward, by considering the yarn count, the area of the yarn bundle sample is determined. Table 1 shows the warp and weft densities of real carpet that are the base items for selecting the yarn densities in the sample bundle. For an easier calculation, it is possible to define a coefficient which is calculated from the ratio of the yarn cross-section area obtained by experimental method to that obtained by theoretical

Table 1—Carpet densities and coefficient calculation [Pile yarn count = 5.5Nm]

Carpet model	Density			Area of yarn cross-section, cm ²		Coefficient (C)
	Warp /cm	Weft /cm	Pile /cm ²	Exp.	Theoret.	
350	3.5	9	63	0.01587		7.86
500	5	10	100	0.01	0.00202	4.95
700	7	10	140	0.0102		5.05

Exp.—Experimental value.
Theoret.—Theoretical value.

method. In this study, the carpet model of 500 has been chosen to achieve this ratio, since it is the conventional carpet density that is used in the global market. Consequently, the coefficient used in this study is taken as 4.95. This means that if the operator calculates the theoretical area of yarn [based on theoretical yarn diameter Eq. (1)] and multiply this number by the coefficient, the occupied area by yarn is obtained (Fig. 2).

The theoretical yarn diameter [$d(cm)$] and theoretical yarn area (S_t) were obtained using the following relationship⁴³:

$$d = \sqrt{\frac{4 \times 10^{-2}}{\rho_{fiber} \times \pi \times N_m}} \quad \dots (1)$$

$$S_t = \frac{\pi \times d_{cm}^2}{4} \quad \dots (2)$$

$$S_A = S_t \times C \quad \dots (3)$$

$$S_{tube} = S_A \times n \quad \dots (4)$$

where S_t and S_A are the theoretical area and occupied area respectively, which are obtained from Eqs (2) and (3) respectively. As previously mentioned, in Eq. (3), coefficient (C) is chosen from Table 1 (C=4.95). If the bundle includes n yarns, the total tube area can be determined from Eq. (4). Table 2 shows the details of calculation for the two assumed tube areas.

2.1.1 Specifications and Number of Bundle Images

The size of taken picture should be as large as that the image analysis technique would be possible via good statistical output. In addition, it would not be so large to have different resolutions in boundaries or to perceive different lights from different sides of the pictures. Achieving the mentioned specifications, a camera with high resolution and wide visibility

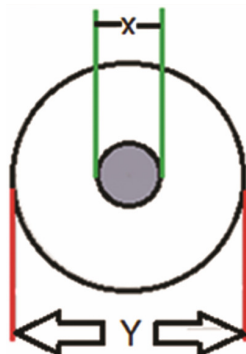


Fig. 2—A yarn, which is located in the bundle [x— yarn theoretical diameter; y— diameter of occupied space]

scope can be used. With good pictures, it is possible to crop a section of the original picture for further analysis. Referring to Fig. 3, the tube shape is not an important matter, but the circular shape is found to be more suitable because mostly the yarn cross-section shape is circular and it captures better fitness inside the tube area.

The number of pixels is very important in the image processing, and is the base in calculating the free space area, number of objects and total area and so on. Naturally, this variable (number of pixels) follows the binomial function because of their discrete nature. However, for n calculated from Eq.(5), it could be counted as a normal distribution⁴⁴. Thus, the number of sample pictures can be obtained from the following equation:

$$n > \max \left\{ 9 \times \frac{p}{q} \text{ or } 9 \times \frac{q}{p} \right\} \quad \dots (5)$$

$$9 \times \frac{q}{p} = 9 \times \frac{0.7}{0.3} = 21$$

$$9 \times \frac{p}{q} = 9 \times \frac{0.3}{0.7} = 3.87 \quad \dots (6)$$

The results indicate that the minimal number of those samples should be 21. However, in this work, for higher confidence, 25 tests were conducted.

2.1.2 Bundle Assembling and Grading Pin-Point Effect

For bundle assembling, it is necessary to make a skein of yarn, and then pull the skein inside the tube using a bent rod. The calculated number of yarns (n) should be placed inside the tube. For example, considering a bundle of 50 turns, the number of yarns

Table 2—Skein turns for two assumed table areas

Coefficient (C)	Pile		Theoretical area cm ²		Number of yarns	Skein turn
	Count	Material density g/cm ³	Pile yarn	Tube		
4.95	3.45	0.9	0.0032	0.950	59.688	29.8440
7.86	5.5	-	0.0507	5.309	13.318	6.6593

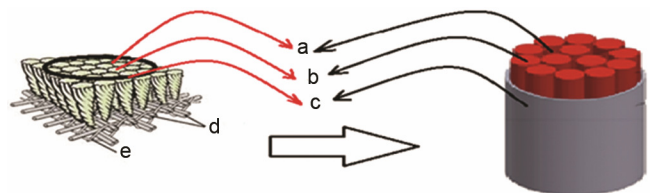


Fig. 3—Schematic diagram of tube positioning around pile yarns (a) free spaces between yarns, (b) pile yarns, (c) assumed tube around the yarns, (d) weft yarn and (e) warp yarns

located in the bundle would be 100. The pin-point index is calculated from the following equation:

$$\text{Pin-point index} = \frac{100 \times \text{free area in bundle}}{\text{(total area in bundle)}} \quad \dots(7)$$

Here the free space is the number of black pixels and the total area would be the image pixels. It is important to compare the pin-point effect of two yarns in different materials or counts. If the yarns were the same, the comparison would be easier. Referring to Eq.(7), the increase in free space in bundle will result in an increase in the degree of pin-point.

2.2 Experimental Tests

The experimental test has been done for BCF (bulkied continuous filaments) polypropylene yarn, while time (in five levels), temperature (in five levels) and twist (in five levels) were changed. The yarn of 1600 den (144 filaments, trilobal filament, MFI 25, 2500 m/min production speed and 1.2% crimp contraction) produced by Swisstex BCF spinning machine was used. Samples were twisted (0, 40, 80, 120, 160 tpm) and heat set at different temperatures [23 (room temperature), 60, 90, 120 and 150°C] and different durations [0 (for raw sample), 30, 60, 90, 120 s]. These domains have also been used in other research works^{2, 4, 16, 21}. A Taguchi L25 orthogonal array was designed with the help of Minitab 16 software to investigate the effect of parameters namely twist, temperature and time, on the pin-point index after the heat setting process. The design of experiments like Taguchi is an engineering approach to optimize the product quality and process conditions, so that they become less sensitive to the causes of variation. It must be noted that studying these parameters using the conventional full factorial method requires 125 runs, but with the Taguchi method, the number of runs is reduced to 25 instead. Hence, Tagouchi Method's⁴⁵ is used for the design of experiments, and finally 25 sets are defined for testing (Table 3). The samples were heat set using an oven with air circulation. This is the same as power heat set machine in the dry mode, while the oven temperature can be controlled with a better accuracy. Afterwards, yarn heat setting, bundle preparation and image acquisition of bundles cross-sections were measured respectively. In all the aforementioned steps, the maximum accuracy is a necessity for attaining the most precise results. For example, in cutting and cross-section preparation, we should design a powerful cutter to achieve immense cut of the surface.

The bundle was placed on the wooden template and images were captured by DINO-Lite2 via ring light including 6 bright LED. The image from the sample was taken in RGB format. Images were taken randomly from different samples. The image capturing was accomplished under the same conditions for all samples. In the developed method, the input image was converted into the binary image with a threshold of 0.5. In the binary images, white and black pixels indicate yarn and background with a value of 1 and 0 respectively. After applying some morphological operations to remove noise from the binary image, such as closing, opening, eroding, dilation and filtering^{31,46,47}, finally pin-point index was captured. Figure 4 depicts the original and processed image. The pin-point index (P.P.I) in the bundle cross-section was calculated (Table 3). According to

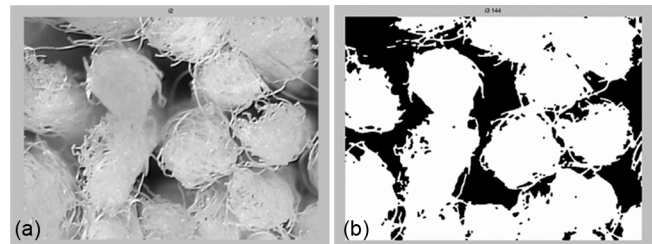


Fig. 4—Yarns bundle (a) origin bundle image and (b) the binary image

Table 3—The degree of pin-point in various bundle samples

Sample code	Twist tpm	Time s	Temperature °C	P.P.I
1	0	0	23	32.06
2	0	30	60	24.55
3	0	60	90	18.91
4	0	90	120	17.74
5	0	120	150	14.83
6	40	30	23	32.72
7	40	60	60	37.42
8	40	90	90	38.52
9	40	120	120	46.39
10	40	0	150	54.08
11	80	60	23	43.49
12	80	90	60	49.61
13	80	120	90	74.87
14	80	0	120	76.92
15	80	30	150	108.81
16	120	90	23	45.93
17	120	120	60	55.01
18	120	0	90	63.5
19	120	30	120	93.39
20	120	60	150	154.3
21	160	120	23	51.15
22	160	0	60	79.22
23	160	30	90	100.4
24	160	60	120	206.6
25	160	90	150	289.75

this table, increase in time and temperature increases the pin-point index of twisted yarns. Subjective evaluation of pin-point effect has been done by expert vision for verification of suggested method⁴⁸.

2.3 Overview of ANFIS and ANN

Jang⁴⁹ presented the ANFIS system which combines both artificial neural network and fuzzy logic. It designed the rules based on the input data, and calculates the weights based on artificial neural network design. It is capable of handling the complex and non-linear problems. The operation of ANFIS looks like feed forward, back-propagation network. Consequent parameters are calculated forward while premise parameters (MFs) are backward. Even if the targets are descriptive, ANFIS may attain the optimum result rapidly. In fact, there are two learning methods in the neural section of the system, viz hybrid learning method and back propagation learning method. An ANFIS gives the mapping relation between the input and the output data by using hybrid learning method to determine the optimal distribution of membership functions (MFs). Both ANN and fuzzy logic (FL) are used in ANFIS architecture. Such structure makes the ANFIS modeling more systematic and less reliant on expert knowledge. The difference between the common neural network and the ANFIS is that, while the former captures the underlying dependency in the form of the trained connection weights, the latter does so by establishing the fuzzy language rules⁵⁰⁻⁵². The ANN models are actually a data processor with several unique advantages, such as no need for simplifying assumptions that can be used with

noisy data or fewer numbers of experimental points and rapid calculation of the response. The ANN model is made of neurons, which are divided into three layers, namely input, hidden, output. Neurons in each layer are connected with associated weights to other neurons in the next layer. The signal is received by the neurons in the input layer and the response in the output layer is calculated through the hidden layers. The available data are divided into two groups, namely training and testing. The first group is used to train the ANN and the testing group is used to control the error during the training process⁵³. Figure 5 (a) and (b) depict the ANN and ANFIS structures with three inputs and one output respectively. The other parameters of the model structure, such as number of neurons and number of hidden layers are defined to achieve good performance of the model.

It should be noted that the performance of the model could be determined with some criteria, such as MSE (mean square error), RMSE (root mean square error) and R² (coefficient of correlation determination).

2.4 Predicting Pin-Point Index

Predicting knowledge is worthy in a wide range of usage. In this usage, it can help the manufacturer and customers to know the pin-point index before running the process to avoid waste in time and energy. As the first step, simple method for drawing the prediction equation has been investigated. Regression equation depicted in following Eq. (8). In this equation, C1, C2, C3, C4 are twist (tpm), time (s), temperature (°C) and pin-point index. It does not show a good correlation [R-Sq = 65.2%

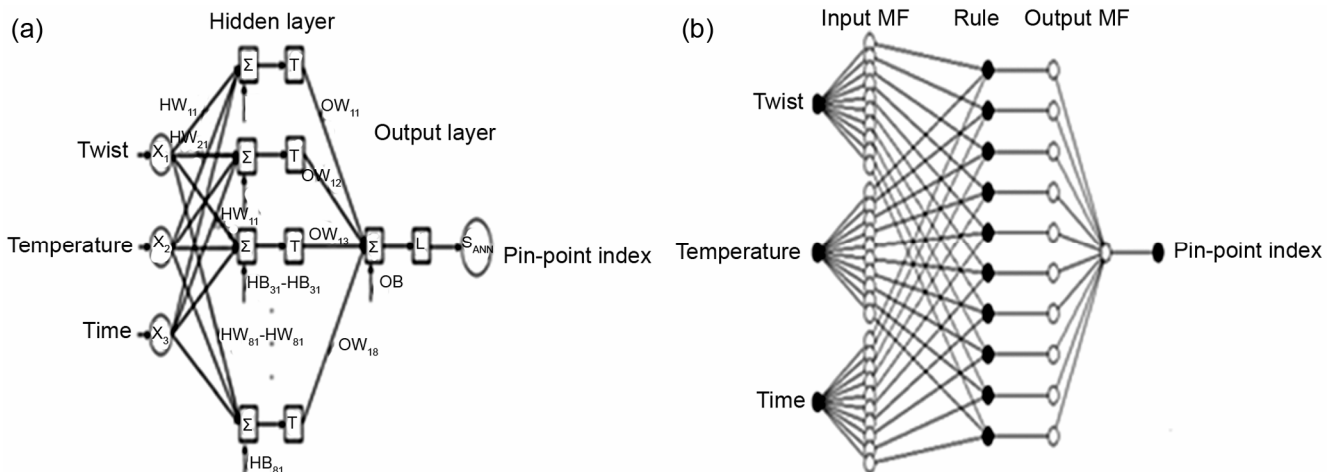


Fig. 5—Models structures (a) ANN model and (b) ANFIS model

R-Sq (adj) = 60.2%] to depict the pin-point index according the input parameters.

$$C4 = - 40.7 + 0.647 C3 - 0.030 C2 + 0.721 C1 \quad \dots(8)$$

Hence, to achieve higher accuracy in the prediction of pin-point index, the other models (ANN and ANFIS) were implemented.

2.4.1 Predicting Pin-point Index using ANN Modeling

There is no rule for determining the number of hidden layer and neurons in each hidden layer for ANN. Thus, in this study, the trial and error method was used to find out the best number of layers and neurons. Regarding the higher number of neurons and layers that make the ANN more complex, and also take more time for the training step, the number of layers and neurons in each hidden layer was considered between 1-5 and 1-20 respectively. In order to determine the optimum number of neurons in the hidden layer, a series of topologies was used. Each topology was repeated ten times to avoid the random correlation due to the random initialization of the weights and bias. The optimal architecture of the ANN model and its parameter variation were determined based on the minimum value of the mean square error (MSE) of the training and testing sets.

Consequently, a multi-layer perceptron ANN with one hidden layer and 6 neurons was used according to Kolmogorov's theorem. "Hyperbolic tangent sigmoid transfer function" in the hidden layer and a linear transfer function in the output node were employed for all the data sets. The data set was split randomly into two sub data sets in order to obtain the most efficient model; for this purpose, 80% was used for model development and adjusting model parameters and the last 20% was used for testing and studying the reliability of the model. The ANN was trained using the scaled conjugate gradient back propagation algorithm (trainscg). In optimization of the ANN model, two neurons were used in the hidden layer as an initial estimate. Finally, RMSE is the minimum while the number of neurons is 6. Hence, the two-layered perceptron ANN model with 6 neurons in the hidden layer has been selected for modeling the pin-point index. The artificial neural network weight matrix (Table 4) can be used to assess the relative importance (RI) of the various input variables in the output variables⁵⁴.

Analyzing Results of ANN Model

The ANN was trained up to 1000 cycles to obtain the optimum weights and bias, and then parameters in the minimized state were saved as the optimum setting of ANN. For calculating the performance of models, the output data of models were rescaled to the original data and then compared with the experimental results. This step (rescaling process) is the same for ANN and ANFIS and then MSE or RMSE is calculated for the test data or some other validation data set. Finally, in cycle 514, the calculated RMSE and MSE values for input test data and target data (experimental data) achieved the minimum level (0.0068 and 4.724e-05 respectively).

2.4.2 Predicting Pin-Point Index using ANFIS Modeling

Adaptive neuro-fuzzy inference system (ANFIS) was employed to predict the pin-point index of pile yarns. Then, the predictive performances of this model were estimated and compared with the proposed ANN model. ANFIS can be considered as a network presentation of a Takagi-Sugenofuzzy inference system⁵², and the if-then rules in Takagi-Sugeno are comprised in the network structure. Two important components of ANFIS are the membership functions and the fuzzy inference rules. Membership function (MF) is a curve that defines how each point in the input space is mapped to a membership value (or degree of membership) between 0 and 1 of the associated fuzzy sets. Fuzzy inference rules are some if-then rules to define the output behavior from the inputs. In ANFIS model, similar to ANN model, to obtain the most efficient model the data set was split randomly into two sub data sets; for this purpose, 80% was used for model

Table 4—Weights and bias obtained in training ANN

Hidden layer			Output layer		
Hidden weight (HW)			Hidden bias (HB)	Output weight (OW)	Output bias (OB)
HW ₁₁	HW ₁₂	HW ₁₃	HB ₁₁	OW ₁₁	OB
-4.9249	-3.1056	-5.2606	7.4509	-0.6309	-3.7038
HW ₂₁	HW ₂₂	HW ₂₃	HB ₂₁	OW ₁₂	
5.0149	-0.4669	2.6572	-1.5309	0.1830	
HW ₃₁	HW ₃₂	HW ₃₃	HB ₃₁	OW ₁₃	
-5.5831	-3.3368	6.689	-3.8847	-1.7340	
HW ₄₁	HW ₄₂	HW ₄₃	HB ₄₁	OW ₁₄	
-1.87716	-0.5124	1.5601	-0.1225	1.7538	
HW ₅₁	HW ₅₂	HW ₅₃	HB ₅₁	OW ₁₅	
-0.22743	2.4707	2.1233	4.2812	2.2588	
HW ₆₁	HW ₆₂	HW ₆₃	HB ₆₁	OW ₁₆	
4.1399	-1.5858	1.6767	5.2486	1.5059	

development and adjusting model parameters and the last 20% was used for testing and studying the reliability of the model. ANFIS simulation was applied by ANFIS toolbox of Matlab software. It is possible to employ different functions to define the base fuzzy inference system, including *gnfis1*, *gnfis2* and *gnfis3*. In this study, all functions have been tested and *gnfis3* is applied due to the better result among the other functions. The advantage of utilizing *gnfis3* methods is good clustering possibility in comparison with *gnfis1*; consequently, it is more time-efficient.

Analyzing Results of ANFIS Model

The ANFIS model runs for 1000 cycles to find the minimum RMSE and the best correlation coefficient. The minimum value of RMSE obtained was 0.004002 in 703th cycle and also the R^2 was 0.999 at this cycle.

3 Results and Discussion

3.1 Analyzing Taguchi Results

The signal to noise ratio is one of the most important indexes for analyzing Taguchi design that has been analyzed for the pin-point index. The signal to noise could be calculated optionally, concerning the goal. Larger is better could be used when the goal is maximizing the response using the following Eq.(9)^{48,55}. In this equation, n denotes the number of observations and Y stands for the measured data, as shown below:

$$S / N = -10 \times \log_{10} \left(\frac{\sum \frac{1}{Y^2}}{n} \right) \quad \dots(9)$$

Better heat setting results in better packing factor for yarns and consequently the pin-point index increases. Therefore, ‘larger is better’ is selected for

the signal to noise analysis. The maximum pin-point index is achieved when the twist and temperature have the maximum level, while the effect on results is not so distinguishable. It is clear that the signal to noise ratio in the middle level of parameters is partly suitable, and may be the optimum value for the commercial use (60 s time, 130°C temperature and 120 tpm twist) for the cost benefit to the factories.

This worthy point of the presented method is the ability to evaluate the differences among the heat set yarns, while shrinkage method cannot detect these differences, because all samples already have shrinkage. On the other hand, shrinkage is a useful parameter when there are raw yarns for testing, while in this method, it is possible to evaluate the heat set yarns without accessing the raw materials by the degree of pin-point indexing system.

3.2 Performance Evaluation

The first step of this research work focuses on defining the pin-point index. Then some models have been developed to predict the pin-point index based on the input parameters. On the other hand, the change in the pin-point index was investigated with the change in twist, time or temperature. Initially a regression model was developed to predict the pin-point index which assigned a low correlation value ($R\text{-Sq} = 65.2\%$). Hence, other models were developed to predict the pin-point index. As depicted in Fig. 6, the $R\text{-Sq}$ for both ANN and ANFIS is very high as compared to regression model. Comparative results between the experimental pin-point index values and the predicted values using the ANN model are presented in Fig. 6. The R^2 value obtained is 0.999, which indicates that the model predicted results shows good fitting with the experimental test data.

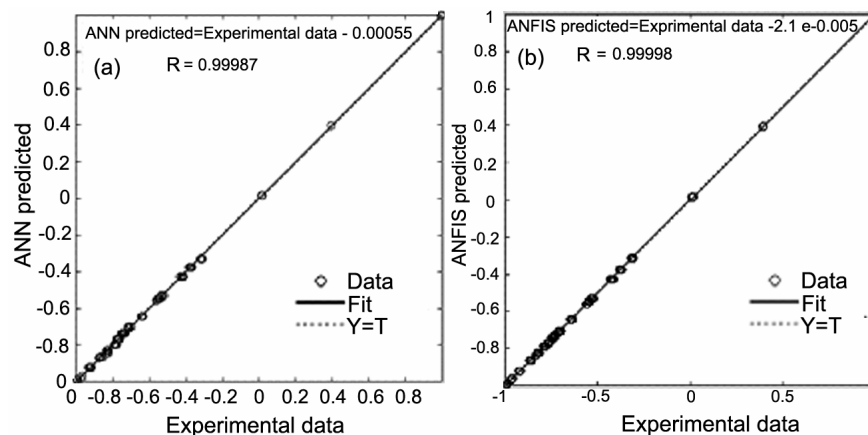


Fig. 6— (a) Regression plot between the target (experimental data) and model output (ANN predicted) and (b) Regression plot between target (experimental data) and model output ANFIS predicted

Table 5—Prediction performance results of model

Code	ANN (Run 514)	ANFIS (Run 703)
MSE	4.72450968e-05	1.60E-05
RMSE	0.006874	0.004002
R ²	0.99987	0.99998
Maximum absolute percentage error	31.5142	22.4694
Minimum absolute percentage error	0.0013	0.0157
STD of absolute percentage error	4.1409	3.8925
Mean absolute percentage error	1.5826	2.3127
Number of error values > 10%	7	2

Also, satisfactory agreement is observed between experimental data and predicted data by the ANFIS model [Fig. 6(b)].

Predict performance and detail results of models are depicted in Table 5. The predict performance of ANFIS is slightly better than that of ANN. The maximum absolute percentage error is 31.5 in the case of ANN, while it is 22.46 for ANFIS model. The range of error is also smaller for ANFIS. Both models demonstrate a good agreement with the experimental values. MSE has good difference to ANN with lower value for ANFIS.

4 Conclusion

In this study, the pin-point index was defined as an index to evaluate the user-friendly effect of the carpet surface after the heat setting process. The accomplished jam structure of yarn brings an attractive appearance on the carpet surface in comparison to the shedding surface. This effect appears due to the change in yarn geometrical structure after shrinkage. The dense structure of yarn creates free spaces among yarns while weft, warp, and pile density are constant in the woven carpets. In the first section, a novel method for evaluating the degree of pin-point in heat set yarns before weaving the carpet was introduced. A standard method for the bundle preparation was presented for producing the identical samples. The samples have been prepared under different heat set conditions and pin-point index is calculated using the image-processing technique. These results show that by increasing the time and temperature, the pin-point index increases with the decrease in diameter, and finally it results in a closer structure for yarns. In addition, two models have been developed for predicting the pin-point index. The experimental data were applied to both ANN and ANFIS models,

to predict the pin-point index as the output parameters and twist, temperature and time as input parameters. The results show that ANFIS predicts that the performance is higher than ANN.

References

- 1 Everaert V, Vanneste M & Ruys L, *UNITEX*, 6 (1999) 26.
- 2 Statton W O, Hearle J W S & Miles LWC, *The Setting of Fibres and Fabrics* (Merrow Publishing, UK), 1971, 1.
- 3 Horrocks A R & Anand S C, *Handbook of Technical Textiles* (Woodhead Publication), 2000.
- 4 Gupta V B, *J Appl Polym Sci*, 83 (2000) 586.
- 5 Seyed Morteza Hossini Z, *Effect of Heat Setting Parameters on Carpet Pile Yarns*, M.Sc thesis, Textile Faculty of AUT, Tehran, 2008.
- 6 Gupta V B, *J Appl Polym Sci*, 83 (2000) 594.
- 7 Gupta V B & Kumar Satish, *J Appl Polym Sci*, 26 (1981) 1877.
- 8 Gupta V B & Kumar S, *J Appl Polym Sci*, 34 (1981) 248.
- 9 Gupta V B & Kumar S, *J Appl Polym Sci*, 12 (1981) 235.
- 10 Lindberg J, Kopke V & Floisand G, *Text Res J*, 34 (1964) 23.
- 11 Baxley R V & Miller R W, *Text Res J*, 61 (1991) 697.
- 12 Shishoo R L & Olofsson B, *J Text Inst*, 60 (1969) 211.
- 13 Pal S K, Mehta Y C & Gandhi R S, *Text Res J*, 59 (1989) 734.
- 14 Cullerton D L, Ellison M S & Aspland J R, *Text Res J*, 60 (1990) 594.
- 15 Vasanthan N, *Text Res J*, 74 (2004) 545.
- 16 Dadgar M, Hosseini Varkiyani S M, *Tekstilna Industrija*, 34(2014)231.
- 17 V B Gupta, *J Appl Polym Sci*, 26 (1981) 12.
- 18 Gupta A K & Maiti A K, *J Appl Polym Sci*, 27 (1982) 56.
- 19 Sardag Sibel, Ozdemir Ozcan & Kara Ismail, *Fibres Text East Eur*, 15 (2007) 70.
- 20 Simal A L O & Martin A R, *J Appl Polym Sci*, 68 (1998) 441.
- 21 Sarkeshick S, Tavanai H, Zarrebini M & Morshed M, *J Text Inst*, 100 (2009) 128.
- 22 Samuels Robert J, *Structured Polymer Properties* (John Wiley & Sons, USA), 1973.
- 23 Lin J-J, *Text Res J*, 77 (2007) 336.
- 24 Wang J & Wood E J, *Text Res J*, 64 (1994) 215.
- 25 Pourdeyhimi B, Sobus J & Xu B, *Text Res J*, 63 (1993) 523.
- 26 Dayiary M, Shaikhzadeh Najar S & Shamsi M, *J Text Inst*, 101 (2010) 488.
- 27 Pourdeyhimi B, Ramanathan R & Javadpour S, *Text Res J*, 64 (1994) 528.
- 28 Wood E J, *Text Res J*, 63 (1993) 580.
- 29 Bugao X, *Text Res J*, 64 (1994) 697.
- 30 Wu Y, Pourdeyhimi B, Spivak S M & Hollies N R S, *Text Res J*, 60 (1990) 673.
- 31 Sobus J, Pourdeyhimi B, Gerde J & Ulcay Y, *Text Res J*, 61 (1991) 557.
- 32 Presley A B, *Cloth Text Res J*, 15 (1997) 235.
- 33 Pourdeyhimi B, Xu B & Nayernouri A, *Text Res J*, 64 (1994) 130.
- 34 Xu B, *Text Res J*, 64 (1994) 697.
- 35 Ucar N & Ertugrul S, *Text Res J*, 72 (2002) 361.
- 36 Majumdar A, *Indian J Fibre Text Res*, 35 (2010) 45.

- 37 Behera B K & Guruprasad R, *J Text Inst*, 103 (2012) 1205.
- 38 Yel E & Yalpir S, *Proc Comp Sci*, 3 (2011) 659.
- 39 Samui B K, Prakasan M P, Chakrabarty D & Mukhopadhyay R, *Rub Chem Technol*, 84 (2011) 565.
- 40 Lin J J, *Text Res J*, 77 (2007) 336.
- 41 Laha A, De L, Dey M & Sarkar S, *Text Res J*, 24 (2007)53.
- 42 Company P H S, *Power-heat-set's compact heatsetting* (Unitex, Germany), 2007, 24.
- 43 Jaouadi M, Msahli S & Sakli F, *J Text Inst*, 98 (2009)21.
- 44 Leaf G A V, *Practical Statistics for the Textile Industry, Part I, Manual of Textile Technology* (The Textile Institute, Manchester), 1987, 876.
- 45 Soon Young Y, Chang Kyu P, Kim H S & Kim S, *Text Res J*, 80 (2010) 1016.
- 46 Lee H S, Hodgson R M & Wood E J, *IEEE Trans PAMI*, 10 (1) (1988) 92.
- 47 Wood E J & Hodgson R M, *Text Res J*, 59 (1989) 1.
- 48 Dadgar M, Hosseini Varkiyani S M & Merati A A, *J Text Inst*, 7 (2015) 34.
- 49 Jang J S R, *IEEE Transactions on Systems, Man Cyber*, 23 (1993) 665.
- 50 Dadgar M, Hosseini Varkiyani S M, Merati A A & Sarkheyli A, *Tekst Indus*, 61 (2013) 16.
- 51 Min L, Mingyu D & Cheng W, *Aut Sci Eng, IEEE*, 7 (2010) 645.
- 52 Ju J & Ryu H, *Fibre Polym*, 7 (2006) 203.
- 53 Rabbi A, Nasouri K, Bahrambeygi H, Shoushtari A M & Babaei M R, *Fibre Polym*, 13 (2012) 1007.
- 54 Nasouri K, Shoushtari A M & Khamforoush M, *Fibre Polym*, 23(2013) 165.
- 55 Dadgar M, Hosseini Varkiyani S M & Merati A A, *J Text Inst*, 106 (2014) 417.